CHAPTER II

EFFECT OF DOPANT ANIONS ON THE PROPERTIES OF CHEMICALLY SYNTHESIZED POLYPYRROLE

Effect of Dopant Anions on the Properties of Chemically Synthesized Polypyrrole

Abstract

Polypyrrole (PPy) was chemically prepared *via* an *in situ* doped polymerization. Seven dopant anions were utilized at a fixed dopant to monomer molar ratio (D/M ratio = 1/12), to stabilize the positive charges on N of pyrrole rings. These dopant anions were found to play important roles on physical, chemical, and electrical properties of PPy as revealed by several techniques, e.g. the scanning electron microscope, the magnetic susceptibility balance, the X-ray photoelectron spectrometer, the X-ray diffractometer, and the custom-made four-point probe conductivity meter. PPys doped with α-naphthalene sulfonate (PPy/A) and β-naphthalene sulfonate (PPy/B) have good pellet appearance, solubility and thermal stability. Their specific conductivity values are as high as 26 and 32 S/cm at the age of ca. two months. Moreover, PPy/A shows an excellent stability in conductivity; its specific conductivity values decreased only 35 % at the age of more than one year whereas that of undoped PPy a decrease of 98 % was found. PPy/A was chemically synthesized at various D/M ratios. The amount of fed dopant affected not only the amount of α-naphthalene sulfonate dopant but also that of co-dopants present, i.e. HSO_4^- and SO_4^{2-} from oxidant, and unknown dopants from environment. These co-dopants influenced the moisture content in PPy matrix and hence the specific conductivity. The D/M ratio giving PPy/A with high specific conductivity is 1/12; it corresponds to the ratio of dopant and to the yielded PPy of about 1/3.

1. Introduction

Conducting organic polymers have been of increasing interest since their discovery [1]. Insulating forms of conducting polymers which have the specific electrical conductivity (σ) less than 10^{-6} S/cm can be converted into conducting forms with σ between 10^{-2} - 10^{5} S/cm by a 'doping process' [2]. To create p-type doped conductive polymers, their insulating forms are oxidized and the positive charges are left behind: these charges are stabilized by dopant anions. Vice versa, to create n-type doped conductive polymers, the insulating forms of polymers are reduced and dopant cations are needed to stabilize the existing positive charges. These unique properties make conductive polymers suitable to various applications, e.g. rechargeable batteries [3], electrochromic displays [4], and sensors [5].

For polypyrrole (PPy), one of the most widely studied amongst many conductive polymers, p-type doped form is the more thermodynamically stable. Various dopant anions can be introduced via either electrochemical or chemical manner. The latter process has the advantage on mass production. The *in-situ* doped polymerization has been recently developed for PPy to introduce a dopant anion into polymer backbone during being polymerized [6]. It provides powdery PPy with better solubility and conductivity as compared with that doped by the two-step method [6]. Utilizing dopants with different chemical structures results in the modification of PPy, e.g. the surface morphology [7], the solubility [8], the moisture content [9], and the degree of water sorption [10]. In this work, we report the effect of dopant types and dopant concentrations on the physical, chemical, and electrical properties of PPy. Seven dopants were introduced into PPy matrix by the *in situ* doped polymerization under the same polymerization conditions. Their chemical, physical, and electrical properties were characterized and reported with those of the undoped and the dedoped PPys which were both synthesized under the absence of a dopant. The dedoped PPy was prepared by treating the undoped PPy with NH_4OH [6].

2. Experimental

2.1 Materials

Pyrrole monomer (AR grade, Fluka) was purified by distillation under the reduced pressure prior to use. Ammonium persulfate, APS (AR grade, Aldrich) was used as the oxidant and *m*-cresol (AR grade, Fluka) was used as the solvent in the film casting; they were commercially available and used without further purification. The dopants used were α-naphthalene sulfonic acid, sodium salt (AR grade, Fluka), β-naphthalene sulfonic acid, sodium salt (AR grade, Fluka), camphor sulfonic acid (AR grade, Fluka), dodecylbenzene sulfonic acid, sodium salt (AR grade, Fluka), ethane sulfonic acid (AR grade, Fluka), perchloric acid (AR grade, Fluka), and *p*-aminobenzoic acid (AR grade, Fluka). These chemicals were used as received.

2.2 The Polymerization Procedure

The doped PPy with various dopant anions were chemically synthesized by the *in situ* doped, oxidative coupling polymerization according to the method of Shen *et al.* [6]. The solution of 0.6846 g (3.0 millimole) ammonium persulfate in 10.0 ml deionized water was slowly added to the mixture of 1.2 millimole of dopant anion and 1.0 ml (14.5 millimole) pyrrole in 20.0 ml deionized water. The reaction was carefully maintained at 0 °C (±0.5 °C) for 2 hours. The contact time between the growing polymer and the oxidant was shortened from the reference method to minimize a possible degradation of PPy. The obtained PPy was precipitated by pouring the reaction mixture into a large excess amount of deionized water. The PPy powder was washed several times with deionized water and methanol before drying in a vacuum at room temperature for 2 days. The undoped PPy was synthesized by the same procedure but in the absence of a dopant anion. The dedoped PPy was prepared by treating undoped PPy with 2 M NH_4OH for 12 hours. The notations used for all PPys are tabulated in Table 1. In order to study effect of molar ratios of dopant anion to pyrrole monomer (D/M ratios) on the properties of PPy, PPy was

synthesized with various amounts of α-naphthalene sulfonic acid, sodium salt. The D/M ratios were chosen to be 1:96, 1:48, 1:24, 1:12, 1:6, 1:3, 1:2, 2:3, and 1:1.

2.3 The Characterizations of PPys

2.3.1 Physical properties

The morphologies of the PPy pellets were studied by using the scanning electron microscope (SEM, JOEL model JOEL 520). The accelerating voltage and the magnification used were 20 kV and 3500 times, respectively. A thermogravimetric analyzer (TGA, Perkin-Elmer model TGA7) was used to determine the moisture content and the onset temperature of PPy degradation. The furnace temperature was varied between 25 to 700 ^{o}C with a heating rate of 10 ^{o}C/min under the N_2 atmosphere. The moisture content was determined from the weight loss of PPy when temperature was increased from 25 to 150 ^{o}C. A X-ray diffractometer (XRD, Rigaku model D/MAX-2000) was used to characterize the order aggregation in amorphous PPy. Samples, in the forms of pellet pressed at 60 kN, having a diameter of 1.3 cm and thickness of ~0.5 mm, were mounted onto metal sample holders. The X-ray source was Cu K-Alpha 1. The diffraction pattern was taken in the 2θ range of 5 – 40 degrees with the scanning speed of 5 degree/min.

2.3.2 Chemical Properties

The functional groups of synthesized PPy were characterized by a Fourier transform infrared spectrometer (FT-IR, Bruker model FRA 106/S). The FT-IR absorption was taken for 20 scans at the wavenumbers between 400-4000 cm^{-1} with the resolution of 4 cm^{-1}. A ultraviolet-visible spectrometer (UV-Vis, Perkins-Elmer model Lambda 16) provided the characterization of charge carrier species. Transparent films of PPys were prepared by means of the solution casting. 1 mg of PPy was dissolved in 20 ml of *m*-cresol. To obtain a completely clear solution, the solution was filtered through a PTFE membrane with the pore size of 1.0 μm. After

smearing this solution onto a glass slide, the solvent was allowed to evaporate in a vacuum oven at 60 °C for 5 hours. Each visible spectrum was taken in the range of 350 – 900 nm with a scan speed of 1440 nm/min. Another instrument used for the investigation of charge carrier species was a magnetic susceptibility balance (MSB, Johnson Matthey Chemicals). The positive value of the corrected molar magnetic susceptibility, $\chi_{corr,M}$ reveals the paramagnetic property of materials [11], e.g. the material containing polaron species. On the other hand, the negative value indicates a diamagnetic property, but it cannot be used to distinguish the bipolaron state from the neutral state. The doping level can be determined by an elemental analyzer (EA, Perkins-Elmer model PE 2400 series II CHNS/O) and the scanning electron microscope (EDS/SEM, JOEL model JOEL 520) in the energy dispersive mode. For PPy doped with sulfur-containing dopant, the apparent doping level is defined as the number of S atoms per 1 atom of N, *S/N*. For PPy doped with perchlorate and PPy doped with *p*-aminobenzoate, it can also be defined as *(S+Cl)/N x 100* and as *[S+1/2 O]/[(N-1/2 O)] x 100%*, respectively. Note that the number of S atoms in PPy doped with a non sulfur-containing dopant is also taken into account because there is the presence of HSO_4^- and SO_4^{2-} acting as the co-dopants [12,13]. The most powerful instrument for the determination of chemical compositions, doping levels, and charge carrier species is the X-ray photoelectron spectrometer (XPS, Perkin Elmer model PHI 5400). The non-monochromatic MgKα with photon energy of 1253.6 eV was selected as the X-ray source. The X-ray source power was 300 W (15 kV x 20 mA). The pass energy used was 17.90 eV. The take-off angle was 45°. The sensitivity factor values for the Omni-Focus Lens A are 0.477 for N 1s and 0.570 for S 2p spectra.

2.3.3 Electrical Properties

In order to study the electrical properties of PPy, 0.05 g of PPy powder was ground and pressed by a hydraulic press at 60 kN into a pellet with the diameter of 2.5 cm and a thickness between 60 – 90 μm. The thickness of each pellet was measured by a thickness gauge (Peacock model PDN 12N) having a resolution of 0.001 mm. The specific conductivity, σ of the PPy pellet was measured by a custom-made four-point probe conductivity meter [13]. Si and SiO_2 sheets with known resistance values were used in the probe calibration. The current, which was applied to the outer terminals of the probe, and the voltage drop between the inner terminals of the probe were detected The suitable current used was determined for each PPy; it was set at a level so that each PPy still had its Ohmic behavior without the Joule heating effect. For instance, the current used for PPy/U and PPy/A was 2 (± 0.5) mA and 20 (± 1) mA, respectively. The specific conductivity values were measured at the age of about two months after they have virtually ceased to changed, and at the age of more than one year to see roughly the electrical stability of each PPys after a long term storage in the ambient pressure, temperature, and humidity.

3. Results and Discussion

3.1 Effect of Dopant Anions

3.1.1 Physical Properties

3.1.1.1 Appearance, Morphology, and Pellet Density

All of PPys, including PPy/U and PPy/De, are black. Notations of various PPys synthesized and doped are listed in Table 1. PPy/A and PPy/B are relatively softer than the others. After they were pressed into pellets, PPy/A and PPy/B pellets turned out to be very shiny and slightly bendable. The pellets of other PPys, especially PPy/U and PPy/De, are on the other hand dull and very brittle. PPy/D

pellet is shiny but very brittle. The physical, chemical and thermal properties investigated are summarized in Table 1. As revealed by SEM, the surface morphologies of all PPy powder are globular (see those of PPy/U and PPy/B in Figures 1a and 1c as examples). The sizes of globules of PPy/A and PPy/B (Figure 1c) are smallest whereas that of PPy/D (Figure 1e) is largest. The surface morphologies of the pellets of PPy/U, PPy/A and PPy/D, are shown in Figures 1b, 1d and 1f, respectively. Their morphologies are similar to those of powder form but appear smoother and denser. The pellet densities, as calculated from the pellet weights and pellet thickness values, are tabulated in Table 1. The density of pellet is lowest for PPy/De and highest for PPy/A, PPy/B, and PPy/AB pellets.

There are correlations between the pellets' appearances, morphologies, and densities. When PPys contain irregular globules, their pellets have lower density, dull and brittle. On the other hand, when PPys contain regular and soft globules, their pellets have higher pellet density, shiny and bendable. The examples of the former case are PPy/De and PPy/U, whereas those of the latter case are PPy/A and PPy/B. The smooth surface of PPy/D pellet shows that the observed big globules of PPy/De in Figure 1e are the crushable aggregates of the very fine PPy particles. Dodecylbenzene sulfonate is an effective surfactant; it provided an effective emulsion polymerization of pyrrole monomer in water. The droplets of pyrrole monomer in water were smaller than those in the polymerization with other dopants, resulting in fine PPy particles. Due to its ultra-fine particle size, PPy/D needed ca. 3 times longer time for filtration with the 0.2 μm membrane. PPy/D pellet also has high density; it is shiny but very brittle due to the failure of particle continuity (see Figure 1f).

Table 1 The notations for the dedoped PPy, the undoped PPy, and the doped PPys with various dopants, along with the moisture content and the onset temperature of degradation of dopants, and the physical properties of PPys: the pellet appearance, the solubility in m-cresol, the moisture content, the onset temperature of degradation ($T_{degrade}$) when D/M ratio was 1/12

Notation of material	Dopant			Pellet appearance	Pellet density (g/cm^3)	Solubility in *m*-cresol	Moisture content (wt %)	$T_{degrade}$ (°C)	Disordering proportion from XRD
	Name	Moisture content (wt%)	$T_{degrade}$(°C)						
PPy/De	(dedoped PPy)	N/A	N/A	very dull and brittle	0.86	Insoluble	10.1	175.1	0.45
PPy/U	(undoped PPy)	N/A	N/A	dull and brittle	0.93 *(0.02)*	Insoluble	4.9 *(0.4)*	222.3 *(7.9)*	0.31 *(0.02)*
PPy/A	α-naphthalene sulfonate	3.2	459.0	very shiny and bendable	1.28	Soluble	3.9 *(0.1)*	249.5 *(0.7)*	0.22 *(0.01)*
PPy/B	β-naphthalene sulfonate	0.3	526.4	very shiny and bendable	1.24 *(0.04)*	Soluble	3.0 *(0.4)*	260.2 *(16.2)*	0.23
PPy/C	camphor sulfonate	4.1	196.3	dull and brittle	1.09	Insoluble	4.8 *(1.2)*	202.9 *(5.0)*	0.26 *(0.03)*
PPy/D	dodecylbenzene sulfonate	3.2	415.0	shiny but very brittle	1.15 *(0.08)*	Soluble	0.9 *(0.1)*	270.9 *(7.1)*	0.24 *(0.03)*
PPy/E	ethane sulfonate	N/A	N/A	dull and brittle	1.03 *(0.03)*	Insoluble	5.6 *(0.7)*	214.8 *(7.6)*	0.24 *(0.02)*
PPy/P	perchlorate	N/A	N/A	dull and brittle	1.11	Insoluble	5.4 *(0.0)*	231.8 *(2.5)*	0.22
PPy/AB	*p*-aminobenzoate	0.7	171.0	shiny but brittle	1.26 *(0.07)*	Insoluble	4.6 *(1.0)*	213.7 *(2.8)*	0.24

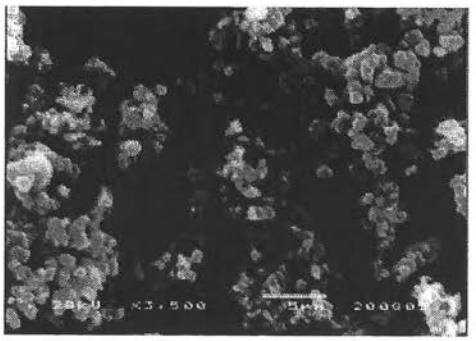

(a)

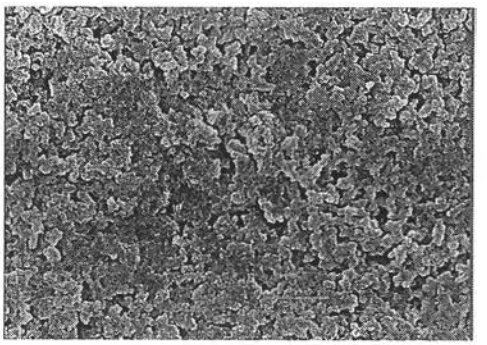

(b)

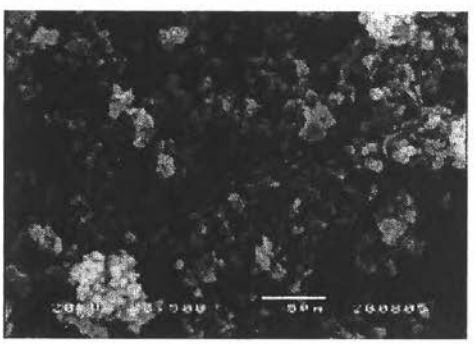

(c)

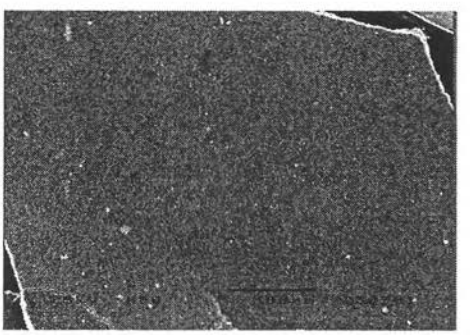

(d)

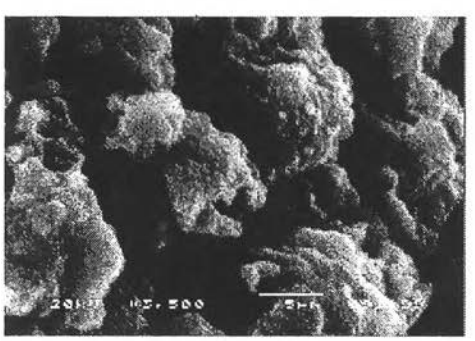

(e)

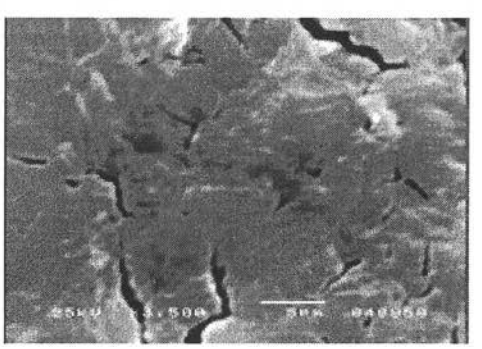

(f)

Figure 1 The scanning electron micrographs of: a) PPy/U powder (3500x); b) PPy/U pellet (3500x); c) PPy/B powder (3500x); d) PPy/A pellet (50x); e) PPy/D powder (3500x); and f) PPy/D pellet (3500x).

3.1.1.2 Solubility

Most of PPys reported in many previous works [6,8] are insoluble in most common solvents. This is believed to be caused by an intense interchain cohesion, high anisotropy of interchain interactions, and/or crosslinking [14]. In *m*-cresol, the good solvent for PPy [6,8], there are only three PPys in this work that are soluble, i.e. PPy/A, PPy/B, and, especially, PPy/D (see Table 1). These three PPys consist of the big aromatic sulfonate dopants (and long alkyl chain for PPy/D) which destroy the interchain interaction between PPy chains and hence increase the solubility of PPy as suggested by Shen [8].

3.1.1.3 Moisture Content

Moisture content values of all PPys are shown in Table 1. The PPy/U, PPy/C, PPy/E, PPy/P, and PPy/AB have approximately the same moisture contents; 4.6-5.6 wt % while the PPy/A, PPy/B, and PPy/D have significantly lower moisture contents; less than 4 wt % whereas PPy/De has the highest moisture content; ca. 10 wt %.

The N-H group in PPy may possibly have the H-bonding interaction with water. The bound water cannot be completely removed at the room temperature [9]. The amount of this bound water in term of moisture content can be affected by the dopant type [9]. The lowest moisture content, which was found in PPy/D, is possibly caused by the long hydrophobic chain of dodecylbenzene sulfonate dopant. Other PPys doped with short chain organic dopants or inorganic dopants have slightly higher moisture contents. The significantly high moisture content in PPy/De could be the result of the additional base treatment in the dedoping process, which was carried out in water. It was noticed that its pellet density is very low; however, there is no clear correlation between moisture content and pellet density.

3.1.1.4 Thermal Stability

Degradation temperatures of all PPys are tabulated in Table 1 along with those of some solid dopants. Comparing with PPy/De, all doped PPys and PPy/U have higher degradation temperatures, especially, PPy/A, PPy/B and PPy/D: they have $T_{degrade}$ higher than 250 °C. These three PPys were doped with the aromatic sulfonate dopants which have the onset of degradation temperature more than 300 °C.

3.1.1.5 Order Aggregation

The X-ray diffractograms of PPy/U and PPy/A as the representative of doped PPys are shown in Figures 2a and 2b, respectively, with their deconvoluted results underneath. All of the PPys exhibit similar X-ray diffractogram; however, there are some differences when examined in detail.

The broad maximum at $2\theta = 25.4 - 27.8^{o}$ corresponds to the d-spacing of 3.2 – 3.5 Å, which is close to the van der Waals distance of the aromatic groups [15]. For all PPys, it can be referred to the distance between the aromatic pyrrole rings in different segments (an interplanar spacing). The breadth of peak has an anti-correlation to the extent of crystal by Scherrer equation [16]. The crystal extent was measured in the direction perpendicular to the plane corresponding to the diffraction peak: it was found to vary between 12 – 15 Å for these PPys. Due to its extremely small crystal size, it is considered as the disorder segment in PPy matrices. The proportions of the disorder peak in PPys are shown in Table 1 as the disorder proportion. PPy/De has the highest disorder proportion whereas PPy/A and PPy/B have the highest order proportions. The proportions of disorder segment polynomially correlate with the pellet density (fit goodness or $R^2 = 0.91$) and the moisture content values ($R^2 = 0.85$). For instance, PPy/D has the largest disorder area; it also has the lowest pellet density and the highest water susceptibility. However, it should be noted again that there is no correlation between the pellet density and the moisture content by any types of regression ($R^2 < 0.65$).

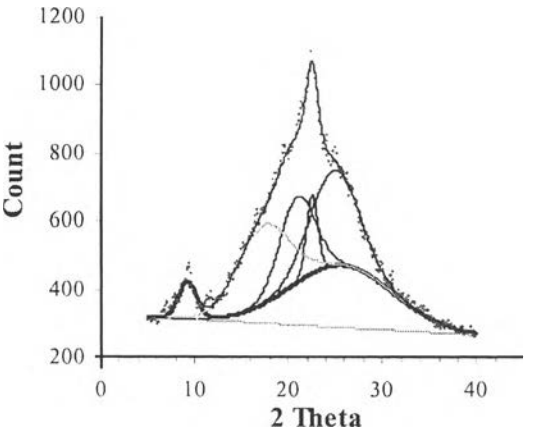

(a)

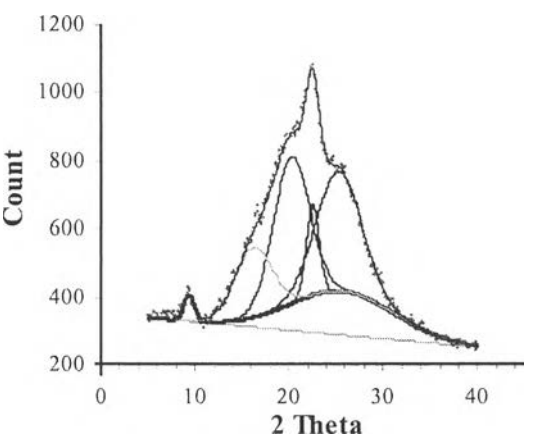

(b)

Figure 2 The X-ray diffractograms of: a) PPy/U pellet; and b) PPy/A pellet, along with their deconvoluted results underneath.

The next broad maxima is located at the same 2θ as the first one but it is sharper and has a more well defined d-spacing (3.5 Å) and its crystal extent is 2 –3 times larger. For the pellets of PPy/A, PPy/B, and PPy/C, the crystal extents are 30 – 34 Å. They are 22 – 28 Å for the others.

The peak locating around 2θ of 22.5 – 22.7° is a very sharp one. It corresponds to d-spacing of 3.9 Å and the crystal size of as high as 99 –125 Å, with no correlation to the dopant sizes. The interpretation for this peak is unclear. It could be the distance between neighboring pyrrole rings in the conjugating system of PPy, where the α-α' linkages are double bonds. Nevertheless, its intensity proportion is very small: 2.1 % for PPy/De, 7.2 % for PPy/D, and 4.9 - 6.5 % for the others. The percentages of these peaks exponentially correlate with the degradation temperatures (R^2 =0.70). This reveals that these double bond linkages built up the hard segments in PPy which induced high thermal stability to PPy.

The next line-broadening at 2θ of 20.0 – 21.0° (d-spacing = 4.2 – 4.4 Å) can be identified as the Miller index of 110 for a hexagonal structure [17] and the distance between neighboring pyrrole rings on the same chain [15] when α-α' linkages are single bonds and flexible. As calculated from its width [16], this type of order consists of 7 - 10 pyrrole rings and has no correlation to dopants.

The low angle peaks in the range of 15.7 - 17.3° corresponds to the distance between two hard segments in PPy backbone which are separated by the counterion molecule. The d-spacing was reported to be affected by the alkyl chain length of the dopants [18]. In this work, it is biggest for PPy/D (5.7 Å) and smallest for PPy/De, PPy/U, and PPy/P (5.1 – 5.2 Å). However, the intensity of this peak is lowest for PPy/D (9.2 %) and highest for PPy/De (14.6 %).

3.1.2 Chemical Properties

3.1.2.1 Functional Groups

The FT-IR spectra of all PPys show nearly the same features (Figure 3). The spectra at the wavenumber higher than 2000 cm^{-1} are featureless due to the presence of an electronic peak at ca. 1 eV or at ca. 8066 cm^{-1} [19]. The peak at 1542-1550 cm^{-1} indicates the C=C stretching vibration [20] while the peak locating between 1033-1045 cm^{-1} identifies the N-H bending of pyrrole unit [21]. There are noticeable differences in PPy metrics due to the presence of the dopant anions. For example, the peak at 1700 cm^{-1} of PPy/AB indicates the stretching vibration of C=O in carboxylic group [22] of the dopant anion, *p*-aminobenzoate. The small peaks at 2919-2923, 2847-2852 cm^{-1} (not shown in Figure 3) in PPy/D and PPy/C belong to the asymmetric and symmetric CH_2 stretching [22] of the long aliphatic chain in the dodecylbenzene sulfonate dopant and of the camphor sulfonate dopant. They are partially covered by the electronic peak. The peak between 1170-1178 cm^{-1}, belonging to asymmetric stretching vibration of SO_2 in non-aromatic sulfonate [23], is present in the spectra of PPy/E and PPy/C. The peak locating around 615-618 cm^{-1} is the characteristic peak of the sulfonate group (v S-O) [13]. It appears in all doped PPy spectra, including the PPys doped with the non-sulfur-containing dopants and the undoped PPy. This indicates the presence of co-dopant, HSO_4^- and SO_4^{2-} from the oxidant used [12,13]. The absence of this peak in PPy/De shows the success of the dedoping process.

3.2.2.2 Nitrogen Compositions

Figure 4 shows the X-ray photoelectron spectrum of PPy/A in the region of N 1s. The main N peak of PPy/A centering at 399.4 eV can be attributed to the neutral N of the pyrrole ring, –NH- [24-27]. The small shoulder at the lower binding energy side can be defined as a structural defect in the form of imine-like nitrogen, =N- [28]. Compared to the position of the main –NH- peak, the shoulder at about 1.5 eV and about 3.1 eV higher binding energy can be attributed to $-NH^{\cdot+}-$ in the polaron charge

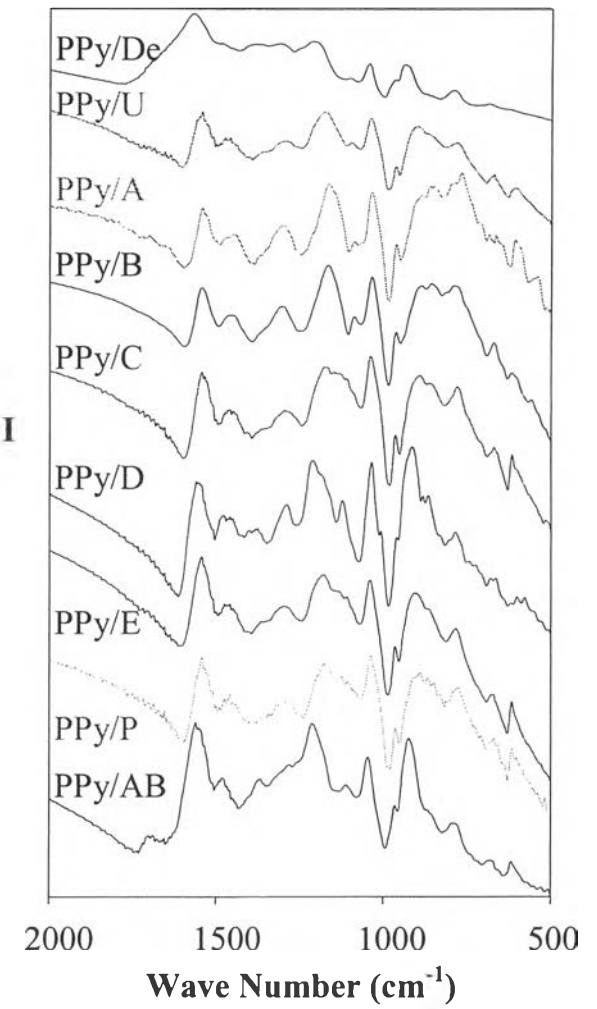

Figure 3 The FT-IR spectra of PPys.

carrier species [29], and to $=NH^{+}$- which is a bipolaron charge carrier species [29], respectively. The compositions of these species are shown in Table 2.

The proportion of imine-like nitrogen defect (=N-) is highest for PPy/De. This was caused by the dedoping process which was carried out in water and air. The proportions of polaron and bipolaron species and the effect of these three species on the specific conductivity are discussed below.

3.1.2.3 Charge Carrier Species

The charge carrier species in PPys as characterized by UV-Vis spectroscopy, MSB, and XPS are shown in Table 2.

The visible spectra were obtained only from the PPys that are soluble in *m*-cresol, i.e. PPy/A, PPy/B and PPy/D: their spectra are shown in Figure 5. The π–π^* transition and the mid-band gap transition of the polaron state correspond to the maximum absorption at about 420 and 650 nm, respectively [6]. The π–π^* transition and the mid-band gap transition of the bipolaron state give the maximum absorption at about 380 and 800 nm, respectively [6]. The visible spectra of PPy/A and PPy/B films clearly show that there are both polaron and bipolaron states as the charge carrier species. Bipolaron state is very dominant in PPy/A film whereas its proportion is small in PPy/B film. In the visible spectrum of PPy/D film, only bipolaron state was observed.

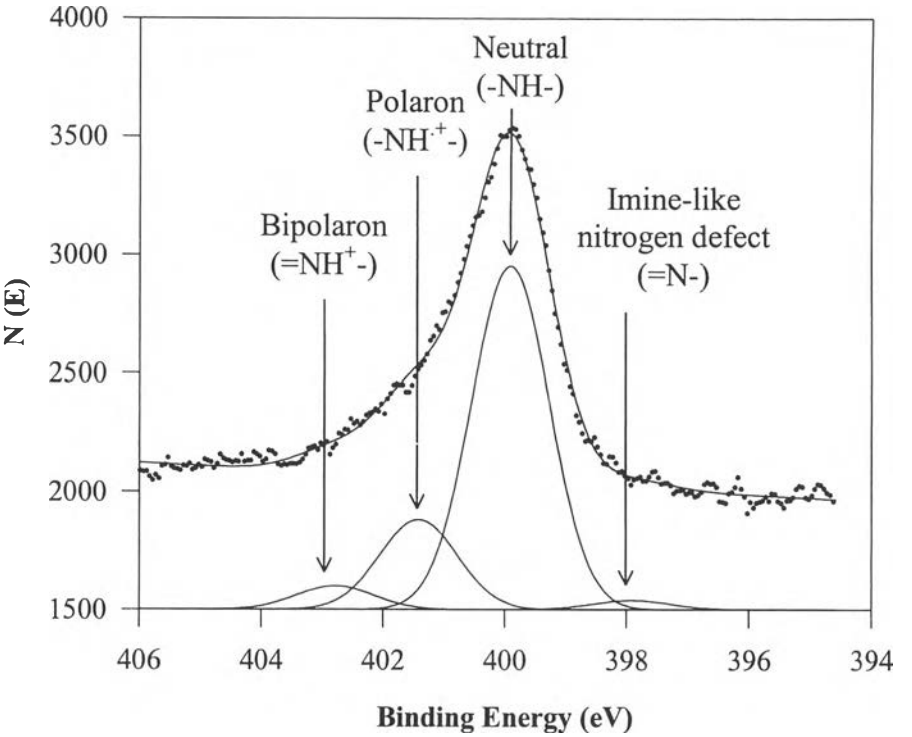

Figure 4 The X-ray photoelectron spectrum of PPy/A in the region of N 1s.

Table 2 The charge carrier species as characterized by UV-Vis, MSB, and XPS techniques (with their proportions) and the doping levels as characterized from EA, SEM/EDS, XPS, in terms of atomic ratio and charge ratio, and the specific conductivity at the age of ca. 2 months and of more than 1 year of the dedoped PPy, the undoped PPy, and the doped PPys with various dopants when fed D/M ratio was 1/12

Material	Proportion of =N- defect	Charge Carrier Species			Doping Level				σ i~2 months (A) (S/cm)	σ i>1 year (B) (S/cm)	(B-A) /A x 100 (%)
		From UV-Vis	From MSB	From XPS	from EA (atomic ratio)	from SEM/EDS (atomic ratio)	from XPS (atomic ratio)	from XPS (charge ratio)			
PPy/De	21.6 *(16.2)*	N/A	Bipolaron or none	Polaron	N/A	0.01 *(0.01)*	0.05	0.12	7.0E-06 *(1.2E-06)*	N/A	N/A
PPy/U	2.8 *(1.0)*	N/A	Bipolaron or none	Polaron	0.12 *(0.01)*	0.11 *(0.01)*	0.12	0.26 *(0.04)*	3.9E+00 *(1.4E+00)*	5.9E-02 *(2.4E-02)*	-9.8E+01
PPy/A	2.2 *(1.4)*	Polaron &Bipolaron	Polaron *(&Bipolaron)*	Polaron, 0.21 &Bipolaron, 0.06	0.24	0.23 *(0.01)*	0.26 *(0.00)*	0.27 *(0.02)*	2.6E+01 *(4.2E+00)*	1.7E+01 *(1.1E+00)*	-3.5E+01
PPy/B	1.4 *(2.1)*	Polaron &Bipolaron	Polaron *(&Bipolaron)*	Polaron, 0.27 &Bipolaron, 0.03	0.26 *(0.00)*	0.24 *(0.02)*	N/A	0.29 *(0.00)*	3.2E+01 *(3.2E+00)*	1.3E+01 *(2.8E+00)*	-5.9E+01
PPy/C	11.6 *(9.7)*	N/A	Polaron *(&Bipolaron)*	Polaron, 0.20 &Bipolaron, 0.02	N/A	0.15 *(0.04)*	N/A	0.22 *(0.02)*	3.3E+00 *(1.1E-01)*	2.6E-01	-8.0E+01
PPy/D	7.2 *(1.7)*	Bipolaron	Bipolaron or none	Polaron, 0.20 &Bipolaron, 0.02	N/A	0.24 *(0.05)*	N/A	0.22 *(0.02)*	1.1E-01 *(7.8E-03)*	9.2E-02 *(5.2E-02)*	-1.6E+01
PPy/E	2.2 *(3.2)*	N/A	Polaron *(&Bipolaron)*	Polaron, 0.21 &Bipolaron, 0.04	N/A	0.13 *(0.05)*	N/A	0.25 *(0.05)*	3.7E+00 *(2.4E-01)*	1.6E-01 *(2.6E-02)*	-9.6E+01
PPy/P	18.5 *(1.2)*	N/A	Polaron *(&Bipolaron)*	Polaron	N/A	0.15 *(0.03)*	N/A	0.20 *(0.01)*	8.4E-01 *(3.3E-02)*	2.9E-01 *(3.3E-02)*	-6.5E+01
PPy/AB	15.8 *(0.8)*	N/A	Polaron *(&Bipolaron)*	Polaron	N/A	0.24 *(0.02)*	N/A	0.14 *(0.02)*	1.7E-03 *(2.1E-04)*	3.7E-05	-9.8E+01

The negative values of $\chi_{corr,M}$ of PPy/De, PPy/U, and PPy/D (see Table 2), reveals the diamagnetic nature and the absence of the polaron species in these PPys. For PPy/D, it confirms the result from UV-Vis technique. PPy/A, PPy/B, and other doped PPys have positive $\chi_{corr,M}$ values. This suggests their paramagnetic nature and confirms the presence of the polaron species in PPy/A and PPy/B revealed by UV-Vis technique. However, the presence of bipolaron which is not detectable by MSB can not be excluded. It is denoted in Table 2 by parentheses.

The charge carrier at the surface of PPy particles can be extracted from the XPS technique which is highly sensitive to surface composition. At the surface of PPy/De, PPy/U, and PPy/D, polaron species were detected; whereas, they are absence in the bulk. For PPy/C, PPy/E, and PPy/AB, XPS techniques shows the presence of the polaron state in their bulks as revealed by MSB. The polaron proportion is highest for PPy/B. The bipolaron species were detected only in PPys doped with the sulfonate dopants: PPy/A, PPy/B, PPy/C, PPy/D, and PPy/E. The results from XPS shows that at the surfaces of PPy/P and PPy/AB, there are only polaron species.

3.1.2.3 Doping Level

The doping levels obtained from EA, SEM/EDS, and XPS are shown in Table 2. Note that EA results correspond to the bulk properties of PPys whereas the other two techniques are surface sensitive and provide the elemental compositions at the surface. XPS provides doping levels both in terms of the atomic ratio of dopant to pyrrole's nitrogen (e.g. S/N for PPy doped with one-sulfur-containing dopant) and the charge ratio (N^+/N).

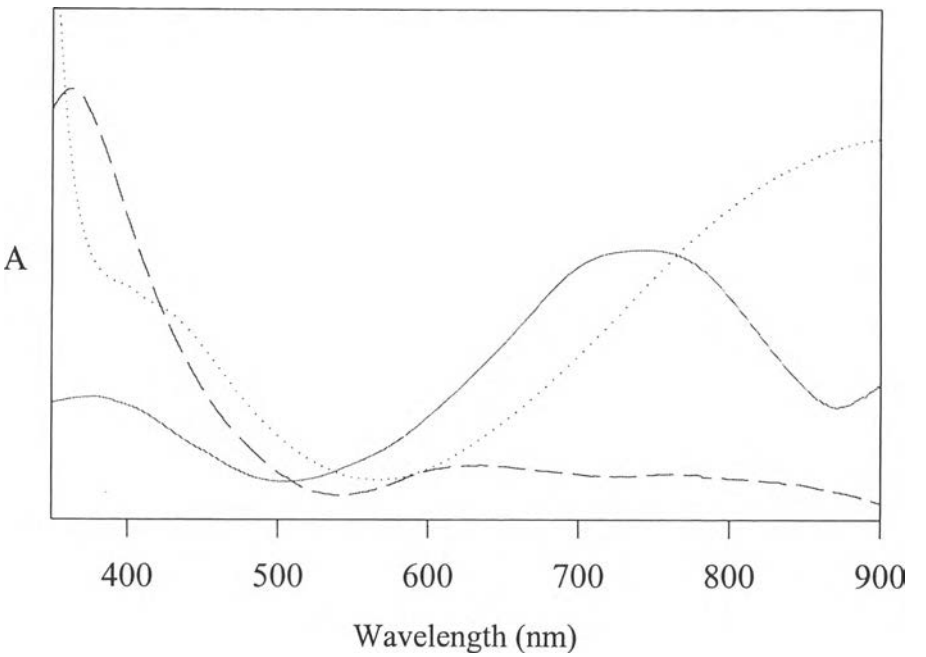

Figure 5 The visible spectra of soluble PPy films cast from *m*-cresol solution: (·····) PPy/A, (– – –) PPy/B, and (——) PPy/D.

For PPy/De, the absence of dopant is confirmed by the S/N value less than 0.05 from EDS and XPS techniques. Nevertheless, the doping level at the surface in terms of N^+/N as revealed by XPS is higher. For PPy/U, the doping level in terms of S/N from EA shows an excellent agreement with that from EDS. However, they are lower than the doping level at the surface in terms of N^+/N from XPS by a factor of two. These suggest the presence of non-sulfur containing co-dopants from environment at the surfaces of PPy/De and PPy/U. For PPy/A and PPy/B, the doping levels of bulk have a good agreement to their surfaces. Moreover, there are good agreements of S/N and N^+/N. These show the high efficiencies of α- and β-naphthalene sulfonate dopants. PPy/D also has a good correlation between S/N and N^+/N, nevertheless, the presence of polaron only at its surface could be derived from presence of HSO_4^- and SO_4^{2-} from oxidant, which provide polaron species only at the surface. In the case of PPy/AB, the atomic ratio of dopant molecule to pyrrole repeating unit is higher than the charge ratio, N^+/N. This indicates the presence of inactive molecules of *p*-aminobenzoate dopant. These molecules do not stabilize the positive charge of PPy but stick onto PPy backbone via the dispersive force attributed from benzene ring and the dipole-dipole interaction attributed from high polar -COOH group. The doping levels in terms of N^+/N of PPy/C, PPy/E, and PPy/P are higher than those expressed in terms of the atomic ratios. This indicates the presence of unknown dopant from environment. The effect of these findings on their specific conductivity values is discussed below.

3.2.3 Electrical Properties

3.2.3.1 Specific Conductivity at the Age of Two Months

Table 2 shows the specific conductivity values of PPys at the age of two months measured in the Ohmic regime of each sample. PPy/De has the specific conductivity as low as 7×10^{-6} S/cm whereas that of PPy/U is ca. six orders of magnitudes higher. Not all of doped PPys have higher specific conductivity than the undoped one. PPy/D and PPy/P have one order of magnitude lower in specific conductivity than PPy/U, whereas that of PPy/AB is as lower as three orders of magnitudes. PPy/C and

PPy/E have approximately the same specific conductivity as PPy/U. The specific conductivity is improved by nearly one order of magnitude when α- or β-naphthalene sulfonates were used as the dopants.

PPy/De has a very low specific conductivity due to the absence of dopant (see Table 2). The introducing of dopant from the environment occurred at its surface where polaron species are found (see Table 2). The presence of co-dopants in PPy/U as discussed earlier corresponds to the unexpectedly high specific conductivity and its black color. When PPy was polymerized under the presence of studied dopants, those co-dopants can be replaced. The α- and β-naphthalene sulfonate dopants can replace them effectively as proved by the very good agreement from the two terms of doping levels: N^+/N and S/N, from all techniques. For PPy/D, even its S/N and N^+/N ratios are approximately the same (see Table 2), the presence of polaron only at its surface indicates a lower of oxidation state at the particle boundaries. This could lead to the failure of electron conduction mechanism and its low conductivity. With the similar doping levels of PPy/C, PPy/E, and PPy/P, they have the specific conductivity in the same order of magnitude as PPy/U. PPy/AB has a very low specific conductivity because the inactive *p*-aminobenzoate molecules interrupt the electrical transportation in PPy as discussed above. For all PPys, the specific conductivity values clearly show the exponential correlation toward N^+/N with R^2 of 0.88.

The existence of =N- defect seems to hinder the specific conductivity of PPy as in the case of PPy/De and PPy/P. However, the exponential correlation between the proportion of =N- defect and the specific conductivity has R^2 of 0.63 only.

3.2.3.2 The Specific Conductivity at the Age of More Than One Year and the Stability in Conductivity

After storage in the ambient pressure, temperature, and humidity, the specific conductivity values of PPys were remeasured at the age of ca. one year. The stability

in conductivity was calculated from the percent change in the specific conductivity from ca. two months to ca. one year, and they are shown in Table 2. Disregarding the PPy/De whose pellets were so brittle such that all them were broken and not usable, PPy/U has the poorest conductivity stability whereas PPy/D has the best conductivity stability. PPy/A and PPy/B have moderately good stability in conductivity.

The stability in conductivity can be directly predicted from difference in doping levels in terms of S/N and N^+/N. When S/N is less than N^+/N, there are unknown dopants from environment that provide only polaron at the surface, leading to the discontinuity of oxidation state at the surface of PPy and finally conductivity decay. This was the case of most PPys, especially PPy/U. On the other hand, when doping levels in terms of S/N and N^+/N are close to each other, PPys tend to have a good stability in conductivity. The examples of this case are PPy/A, PPy/B, and PPy/D.

3.2 Effect of Dopant to Monomer Molar Ratios

Since there is no significant change in many properties of PPy/A at various dopant to monomer molar ratios (D/M ratios), only some changes in properties are discussed here.

3.2.1 Physical Property: Moisture Content

When the D/M ratio is increased from 0/1 (PPy/U) to 1/1, the moisture contents are slightly decreased from 5.6 wt % to 1.4 wt % (see Figure 6). Because there is no significant difference in order aggregation of PPy/A with various D/M ratios, this moisture content decrease could be explained by the increase of co-dopants which are hydrophobic (see below).

3.2.2 Chemical Property: Doping Level

For PPy/A, the doping level was determined from two expressions: N^+/N and S/N, and by two different techniques; XPS and EA. Figure 7a shows the doping levels of PPy/A as a function of fed D/M. Because the amount of the yielded PPy directly depends on the amount of fed oxidant, according to our unpublished data, not on the amount of fed monomer, the ratio of dopant to oxidant (D/APS ratio) is worth discussing and is included in this figure. The doping levels in terms of N^+/N from XPS agree well with those from EA, which was determined for only some samples. As the D/M ratio increases, the doping level in terms of S/N increases and reaches the saturated value at 0.30 –0.35 when D/M ratio is 1/6 and when D/APS is very close to unity. Meanwhile, the doping level in terms of N^+/N remains steady between 0.24 – 0.27 within the whole range of fed D/M ratio. The difference in the binding energy of S IV and S VI [30] allows us to distinguish the α-naphthalene sulfonate dopant (S IV) and the HSO_4^- and SO_4^{2-} co-dopants (S VI). The results are shown in Figure 7b as a function of D/M ratios. In PPy/U (D/M = 0), there is no S IV: there is only S VI of co-dopants. In the presence of α-naphthalene sulfonate even at a very small amount; e.g. 1/96, it exists as dopant, replacing the co-dopants. Amounts of both dopant and co-dopants are slightly increased and levels off as the same trend as the amount of total S in Figure 7a. The ratio of co-dopants to dopant is varied from 1/4 to nearly unity and it seems to be uncontrollable when the D/M ratio is higher than 1/6.

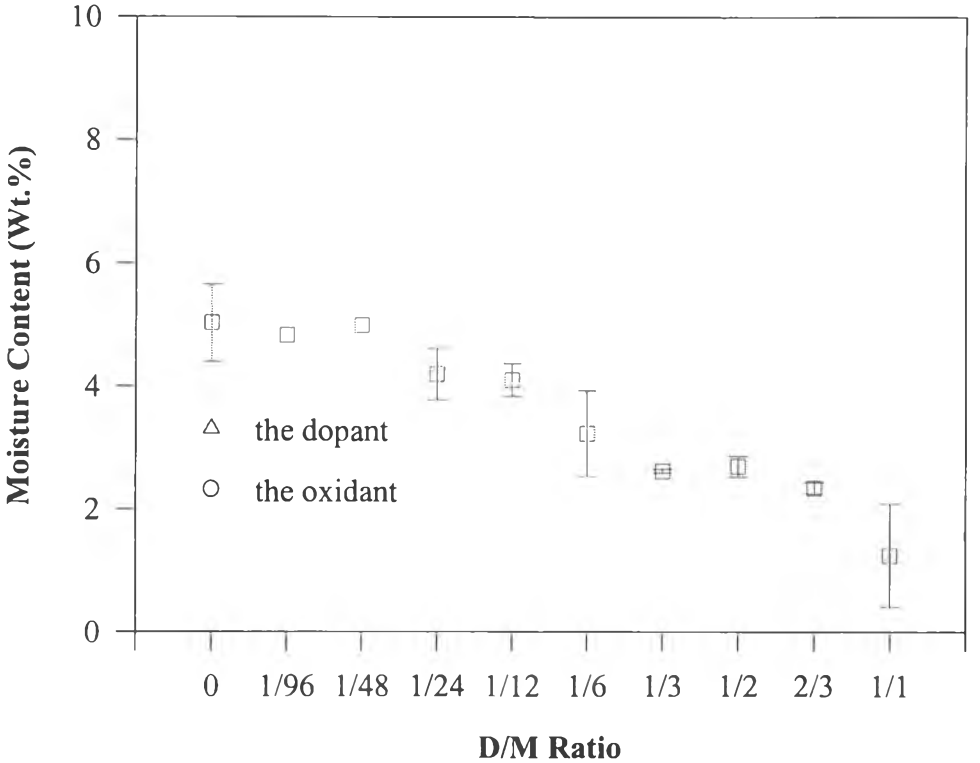

Figure 6 The moisture content of: (□) PPy/A at various D/M ratios; (△) α-naphthalene sulfonate (the dopant); and (○) APS (the oxidant).

The good agreement between S/N data from XPS, which is the surface sensitive technique, and S/N data from EA, which contains information of the bulk, indicates a good distribution of sulfur-containing dopants in PPy/A matrices. The excess amount of N^+/N over S/N at low D/M ratios informs the presence of non-sulfur-containing dopants. When higher D/M ratios is utilized during polymerization, α-naphthalene sulfonate dopant can replace not only co-dopants from oxidant (see Figure 7b), but also those unknown dopants (see Figure 7a). However, at D/M ratios higher than 1/12, S/N exceeded N^+/N and the ratio of co-dopants to dopant seems uncontrollable. These are due to the being overwhelmed of the dopant molecules in the reactor during polymerization. The increase in amount of S VI of co-dopants from oxidant (Figure 7b) corresponds to the decrease of the moisture content as the D/M ratio increases. These co-dopants are inorganic and APS itself has very low moisture content (see Figure 6).

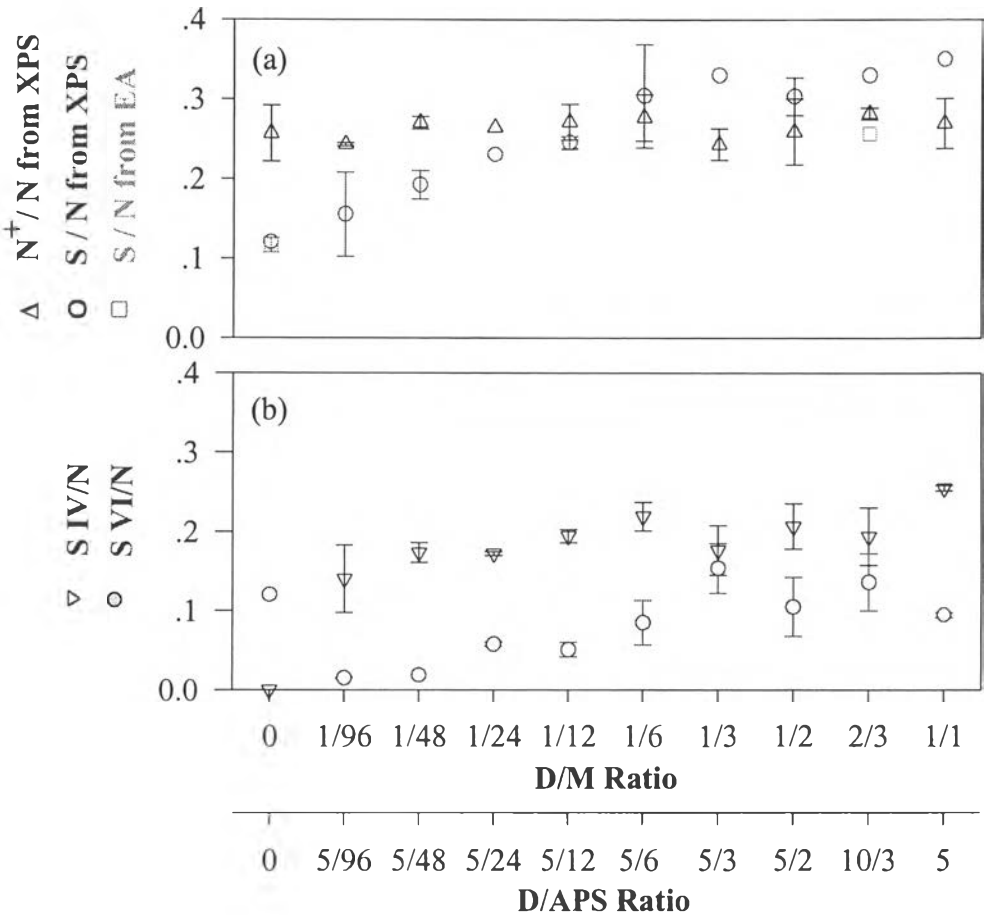

Figure 7 a) The doping levels in terms of: (△) N^+/N and (○) (S IV & S VI)/N from XPS; and (□) S/N from EA of PPy/A as a function of fed D/M ratios and D/APS ratios: and b) the ratios of (▽) S IV and (●) S VI toward N.

3.2.3 Electrical Properties

3.2.3.1 Electrical Conductivity at the Age of Two Months

As seen in Figure 8, the specific conductivity of PPy/A with increasing D/M ratios firstly increases from 3 (PPy/U) to 26 S/cm at D/M ratio of 1/48. It then remains constant until D/M exceeds 1/12: the specific conductivity drops down to be around 10 S/cm.

The change in the specific conductivity as the D/M ratio was varied can be explained by considering the doping levels in Figure 7. At the D/M ratios less than 1/48, the specific conductivity increases due to the increase of α-naphthalene sulfonate dopant which provides a better charge stabilization and higher conductivity. Beyond D/M ratio of 1/24, the specific conductivity does not increase further because the doping level is very close to the stable value, 0.25 (see Figure 7) [31]. The decrease in the specific conductivity is evident when D/M ratio is higher than 1/12 and when S/N is slightly higher than N^+/N (see Figure 7). There is an excess amount of dopant which does not act as a charge stabilizer, and hinder the conductivity. The D/M ratio of 1/12 corresponds to the D/APS or dopant to yield ratio of ca. 1/3: this is consistent with that reported by the chemical analysis of PPy/ClO_4 [32].

3.2.3.2 The Specific Conductivity at the Age of More Than One Year and the Stability in Conductivity

The specific conductivity values of PPy/A at various D/M ratios measured at the age of more than one year are shown in Figure 8. This set of data shows the same trend but with less specific conductivity than those of PPy/A at the age of two months. As considered from the decrement of specific conductivity, when the ratio of α-naphthalene sulfonate dopant to pyrrole monomer or D/M ratio increases from 0 to 1/12, the stability in conductivity is improved. Beyond this D/M ratio, the stability is

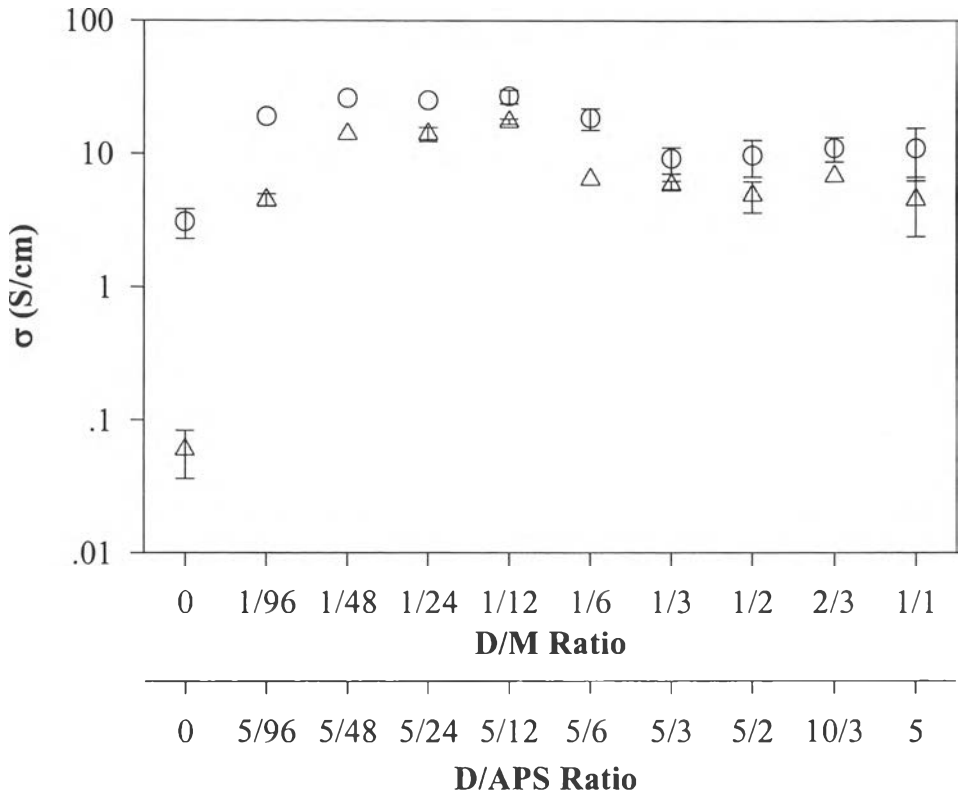

Figure 8 The specific conductivity of PPy/A at various D/M ratios and D/APS ratios, measured at the age of: (○) two months and (△) more than one year.

varied between 35 – 65 % based on the specific conductivity at the age of two months.

4. Conclusion

Among seven dopants used in this work, the α-naphthalene sulfonate and the β-naphthalene sulfonate are the most effective ones for PPy. They provide PPy with the best mechanical, chemical and electrical properties. Even though the dodecylbenzene sulfonate effectively dopes PPy, it provides the ultra-fine PPy particles and the large surface area for the oxidative species in the environment: these lead to the failures in many properties. The *p*-aminobenzoate is the most ineffective dopant. Its inactive molecules are stuck in the matrix of PPy/AB and hinder the electron transportation. At a very low D/M ratio, e.g. 1/96, there was no sufficient amount of dopant to stabilize the positive charges in PPy. Then unknown species from the environment act as co-dopants. With increasing D/M ratio, PPy has better electrical properties due to the presence of the effective α-naphthalene sulfonate dopant. The maximum doping level in terms of N^+/N is 0.24 - 0.27. The D/M ratio giving PPy/A with high specific conductivity and high stability is 1/12; it corresponds to the ratio of dopant and to the yielded PPy of about 1/3. Beyond this D/M value, the dopant molecules become overwhelmed and hinder the electron conduction mechanism. The best PPy is expected to provide the unique properties, e.g. for the sensor technology which will be consequently reported by our group.

5. Acknowledgements

The authors are grateful to all financial supports: the Rajadapisek Fund of Chulalongkorn University; a RGJ grant from Thailand Research Fund, no. PHD/4/2541; and a BGJ award, no. BGJ/5/2543. We are indebted to staff of the Petroleum and Petrochemical College, Chulalongkorn University, Thailand and the staff of the Electron Microscope Analysis Laboratory, the University of Michigan, USA.

6. References

1. J. O'M. Bockris, D. Miller, in L. Alcácer (Ed), Conducting Polymers: Special Applications, D. Reidel Publishing Company, Boston, 1986, p. 1-4.
2. R.S. Kohlman, A.J. Epstein, Insulator-Metal Transition and Inhomogeneous Metallic State in Conducting Polymers, in T.A. Skotheim, R.L. Elsenbaumer, J.R. Reynolds (Eds), Handbook of Conducting Polymers, Marcel Dekker, Inc., New York, 1998, p. 85-86.
3. K. Kaneto, M. Maxfield, D.P. Nairns, A.G. MacDiarmid, A.J. Heeger, J.Chem. Soc., Faraday Trans. 1, 78 (1982) 3417.
4. S. Kuwabata, H. Yoneyama, H. Tamura, Bull. Chem. Soc. Jpn. 57 (1984) 2247.
5. T. Hanawa, S. Kuwabata, H. Yoneyama, J.Chem. Soc., Faraday Trans.1, 84 (5) (1988) 1587.
6. Y. Shen, M. Wan, J. Polym. Sci. Part A-Polym. Chem. 35 (1997) 3689.
7. P. Topart, M. Josowicz, J. Phys. Chem. 96 (1992) 7824.
8. Y. Shen, M. Wan, Synth. Met. 96 (1998) 127.
9. C. Cassignol, P. Oliver, A. J. Ricard, Appl. Polym. Sci. 70 (1998) 1567.
10. H. Okuzaki, K. Takamitsu, T. Kunugi, Polym. 40 (1999) 995.
11. W.L. Jolly, The Synthesis and Characterixation of Inorganic Compounds, Prentice-Hall, Inc., N.J., 1970, p. 370.
12. M.M. Ayad, J. Appl. Polym. Sci., 53 (1994) 1331.
13. W. Prissanaroon, L. Ruangchuay, A. Sirivat, J. Schwank, Synth. Met. 114 (2000) 65.
14. R. Qian, in Conjugated Polymers and Related Materials, W.R. Salaneck, I. Lundstrom, B. Ranby (Eds), Oxford University Press, London, 1993, p. 161.
15. F. Gassner, S. Graf, A. Merz, Synth. Met. 87 (1997) 75.
16. D. Campbell, J.R. White, Polymer Characterization, 2nd ed. Great Britain at the University Press, Cambridge, 1991, p. 163.
17. R.G. Davidson, L.C. Hammond, T.G. Turner, A.R. Wilson, Synth. Met. 81 (1996) 1.

18. W. Wernet, M. Mondenbusch, G. Wegner, Makromol. Chem., Rapid Commum. 5 (1984) 157.
19. G.B. Street, S.E. Lindsey, A.I. Nazzal, K.J. Wynne, Mol. Cryst. Liq. Cryst. 118 (1985) 137.
20. V.-T. Truong, B.C. Terrence, T.G. Turner, C.M. Jenden, Polym. Internal. 27 (1997) 187.
21. B. Tian, G. Zerbi, J. Chem. Phys. 94 (1990) 3886.
22. R.M. Silverstein, Spectrometric indentification of organic compounds, John Wiley & Sons, New York, 1991, p. 117.
23. The Aldrich Library of FT-IR spectra vol. 1, 1997, p. 1491.
24. P. Pfluger, M. Krounbi, G.B. Street, G. Weiser, J. Chem. Phys. 78 (1983) 3212.
25. P. Pfluger, G.B. Street, J. Chem. Phys. 80 (1984) 544.
26. R. Erlandsson, O. Inganas, I. Lundstrom, W.R. Salaneck, Synth. Met. 10 (1985) 303.
27. J.G. Eaves, H.S. Munro, D. Parker, Polym. Commum. 28 (1987) 39.
28. T.A. Skotheim, M.I. Florit, A. Melo, W.E. O'Grady, Phys. Rev. B 30 (1984) 4846.
29. C. Malitesta, I. Losito, L. Sabbatini, P. G. Zambonin, J. of Electron Spectroscopy and Related Phenomena 76 (1995) 629.
30. M. Descostes, F. Mercier, N. Thromat, C. Beaucaire, M. Gautier-Soyer, Appl. Surf. Sci. 165 (2000) 288.
31. M. Salmon, A.F. Diaz, A.J. Logan, M. Krounbi, J. Bargon, Mol. Cryst. Liq. Cryst. 83 (1982) 265.
32. G.B. Street, T.C. Clarke, M. Krounbi, K. Kanazawa, V. Lee, P. Pfluger, J. C. Scott, B. Weiser, Mol. Cryst. Liq. Cryst. 83 (1982) 253.